Climate Dynamics (1987) 2:117-126

Climate Dynamics

GCM studies of the African summer monsoon

LM Druyan*

Sigma Data Services Corp., NASA Goddard Spaceflight Center, Institute for Space Studies, New York, N Y 10025, USA

Abstract. A 37-year simulation of global climate by a 9-level GCM on an $8° \times 10°$ grid showed realistic interannual variation of the computed precipitation over the African Sahel. The model includes an interactive ocean so that interannual variations of sea-surface temperature (SST) also occur. Comparison of an ensemble of five summers that were rainy over the Sahel with five summers of simulated drought showed that insufficient ambient moisture was the immediate cause of the lack of moist convection. The drier conditions are shown to result from weaker moisture advection over the southeast Atlantic Ocean. Weaker southerly winds there and lower sea-level pressure gradients seemed to result from anomalously warm SST. Such SST anomalies have been linked to Sahelian drought in previous observational studies. These regional circulations that were conducive to lower rainfall rates during the north African summer monsoon were not manifestations of the more generalized zonal mean circulation.

1 Introduction

A number of studies have dealt with the circulation characteristics during especially dry summers over the African Sahel in comparison with conditions during rainy summers (Nicholson 1981; Newell and Kidson 1983; Lamb 1978; Kidson 1977). A number of tentative conclusions have been proposed, but the evaluations were limited by the type, resolution and quality of observational data available for the years of particular interest. Climate simulations by a GCM have the advantage of providing complete coverage of all relevant meteorological variables which can be internally summarized by convenient statistics or represented graphically as desired. Follard et al. (1986) give a brief summary of a GCM study that links sea-surface temperatures (SST) with summer rainfall over North Africa by prescribing anomalous SST instead of climatological values. In this and other studies, the response of the GCM to prescribed changes in initial atmospheric state or boundary conditions is taken as an indication of how the atmosphere should evolve under the same influences. Of course, GCM solutions are only approximations of actual atmospheric processes. Moreover, experiments testing the effect of prescribed SST anomalies often cannot account for any ocean response to atmospheric forcing, so that important feedbacks are not simulated. Application of the GCM in researching the synoptics of drought can still be fruitful, however, if the simulations reasonably reproduce observed climates. Dry/wet cycles over particular regions computed in multi- year simulations have not been described in the literature.

This research evaluates some results obtained from the model II version of the GCM used for climate research at the Goddard Institute for Space Studies (GISS). The model has been described by Hansen at al. (1983) and has been applied to a number of studies, e. g., Hansen et al. (1984), Druyan (1982a, b), Chervin and Druyan (1984) and Stone and Chervin (1984). The GISS model II solves the simultaneous equations for the conservation of energy, momentum, mass and water vapor and the equation of state on a coarse grid with horizontal resolution 8° latitude by 10° longitude within nine vertical layers. Physical processes contained in the model include solar and terrestrial radiation transfer; vertical trans-

* On leave from Dept. of Geography, Bar Ilan University, Israel

port of moisture, sensible heat and momentum by convection; clouds from supersaturation and convection; heat and moisture storage in the ground surface; and vertical transport of latent and sensible heat from the surface. In the parameterization of moist convective instability, moist static energy is conserved by rising parcels and mixing of mass with lower levels compensates for upward mass flux. Previously condensed moisture is permitted to reevaporate when unsaturated lower layers are encountered.

A version with interactive ocean was used as the control for an experiment evaluating the consequences of doubled CO_2 concentrations (Hansen et al. 1984) and was run for 37 model years. No prescribed changes were introduced during the 37-year simulation and all changes in boundary conditions were internally computed according to model parameterizations. Ocean temperatures were computed based on specified ocean heat transports and computations of energy exchange between the atmosphere and the ocean mixed layer. The transports and mixed layer depths vary geographically and seasonally and compare well with climatological values. Ocean heat transports were obtained from the divergence of heat implied by energy conservation at each grid box in the standard model II version that uses specified SST. Details and an evaluation of the computations are given by Miller et al. (1983).

Mean summertime monthly precipitation rates saved for the Sahel (here defined as the model grid boxes along 12° N at the longitudes 0°, 10° E, 20° E and 30° E) showed considerable interannual variation (Fig. 1). These simulated cycles of drought and copious rainfall have a variability (standard deviation/mean) of about 16%, while actual (annual) precipitation variabilities along 12° N over Africa (Nicholson 1980) are somewhat higher, 20%—40%, since they are computed from individual station data. Because of the convenience in studying the synoptics of drought via a GCM, monthly means of several synoptic fields were compared for dry and rainy summer months over north Africa.

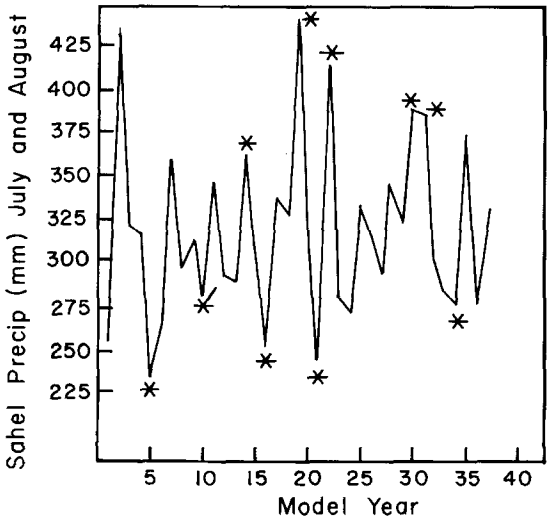

Fig. 1. The July and August precipitation (mm) averaged over the four grid boxes along 12° N, 0—30° E (Sahel) for each of 37 model years. Model years selected for the present study are indicated by *asterisks*

Five model August months with copious Sahelian rainfall (WET), and five with scant rainfall (DRY) were selected from the computed climate history from model years 3—37 and are indicated on Fig. 1. Kidson (1977) justifies basing an analysis of the synoptics of Sahelian drought on August data since the region's rainfall peaks during that month. Moreover, Dennett et al. (1985) show that Sahelian drought can usually be attributed to poor August rainfalls. Nevertheless, the synoptic circumstances leading up to a dry summer may well be apparent during the spring or earlier. Therefore, seasonal and monthly means of precipitation, surface air and sea-surface temperature, sea-level pressure (SLP), resultant surface wind, surface specific humidity and surface moisture convergence were prepared for the WET and DRY ensembles for the months January—August in order to study their synoptic differences. These data were contoured or represented vectorally and were studied using video displays and hard copy plots.

2 August synoptic fields

Horizontal contour and vector representations of August mean computed meteorological variables are analyzed to determine if they reflect distinctly different characteristics during the simulated Sahel droughts, as compared with non-drought conditions.

a) Rainfall

Figure 2 shows the two August ensemble mean rainfall distributions over Africa and the difference field. The distribution for the rainy ensemble is suggestive of the long-term mean pattern (Fig. 2d), except over the coast of west Africa and along the northern edge of the rainbelt that is too

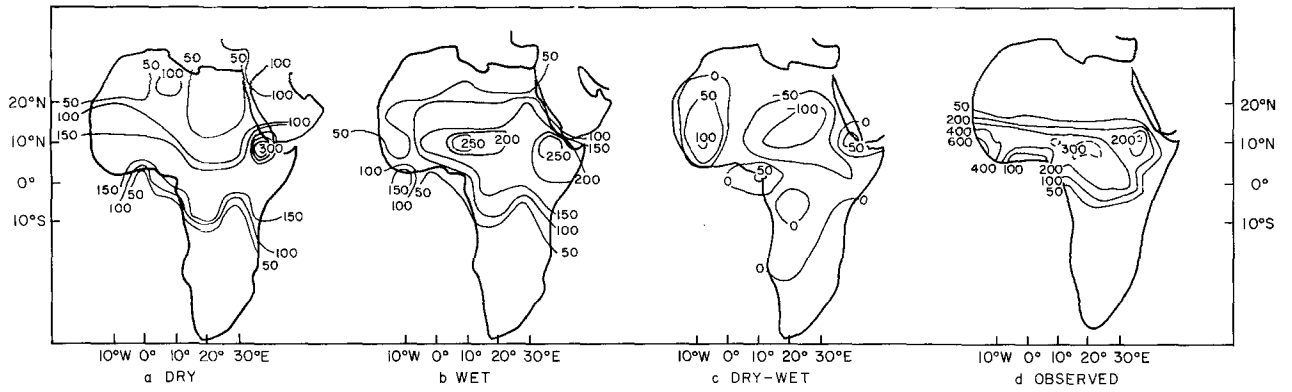

Fig. 2a—d. August mean precipitation (mm): **a** mean of 5 DRY model years; **b** mean of 5 WET model years; **c** DRY-WET differences; **d** observed

diffuse in the model solution. The Sahel (12° N, 0—30° E) receives 39% less rainfall in the modeled drought than in the WET ensemble. Moreover, the WET ensemble mean is 1.5 standard deviations greater than the model's 37-year August mean rainfall for the Sahel, while the corresponding DRY ensemble mean is 1.3 standard deviations less (than the 37-year mean). Along 20° N the deficit is even greater, reaching 120 mm in the area of the Sudan and Chad. The axis of maximum precipitation shifts southward in model drought years, but the suggestion that drought in the Sahel is compensated by anomalously rainy conditions over equatorial regions is not supported by these model simulations. All but one of the individual August rainfall distributions show the east-west isohyetal gradient over north Africa that is so pronounced on the ensemble mean fields. The exception is August of year 34 for which the isohyets along 12° N are rather zonal and the precipitation minimum is at 10° E instead of the usual 20° E location. In the case of the most extreme model "drought" over north Africa (year 21), a broad area centered over 12° N, 20° E received less than 15 mm of rain during August.

Nicholson (1980) describes several spatial distributions of precipitation anomalies that occur during wet and dry years over north Africa. Her type 3 composite (observed in 1910, 1937, 1940, 1944, 1945, 1947, 1966) shows below normal rainfall, except along the northwest coast, similar to the DRY ensemble of the present study. Patterns with the reverse sign, similar to the WET ensemble, were observed in 1933 and 1957.

Teleconnections between precipitation anomalies over Africa and elsewhere were not apparent from the global difference map, except for negative DRY-WET ensemble differences of up to 90 mm over the western Indian Ocean at 4° N and the central Pacific Ocean at 4° S.

b) Sea-level pressure

The August mean sea-level pressure (SLP) over Africa and the adjacent Atlantic Ocean is shown for the two ensembles, together with the SLP difference field, in Fig. 3. SLP values were slightly higher for the drought ensemble over the western Sahara and Sahel but significantly lower over northeastern Africa. As a result, there was an east-west gradient along 20° N within the Intertropical Discontinuity (ITD) trough and to its north in this ensemble, but not in the other. The lower pressures are associated with high temperatures caused by large amounts of insolation reaching the surface during more frequent cloudless periods.

c) Cloudiness

The distribution of August cloud cover for the two ensembles indeed indicates that most of the Sahel and sub-Sahara was much less often cloudy during the simulated drought (not shown). Values averaged about 35% over the eastern Sahel and even less farther north. In the WET ensemble, the model atmosphere was cloudy about 71% of the time along 12° N over Africa.

d) Surface air temperature

Figure 4 shows the ensemble averages of the (August mean) computed surface air temperature.

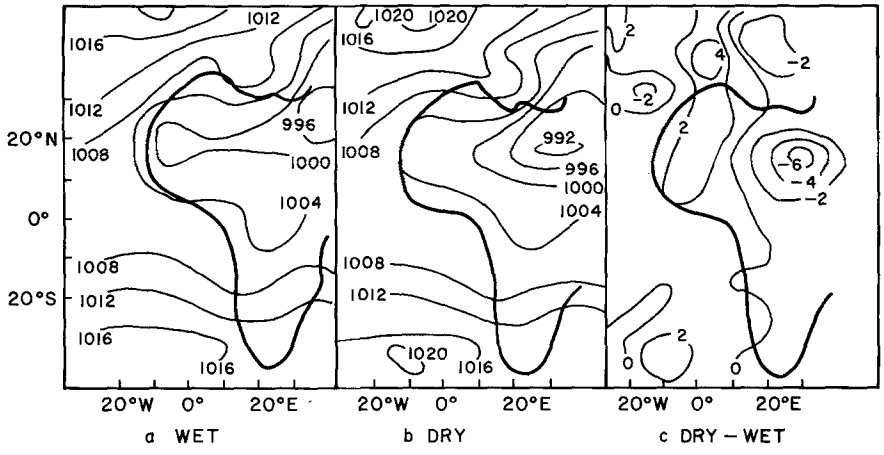

Fig. 3a—c. August mean sea-level pressure (mb): **a** WET ensemble; **b** DRY ensemble; **c** DRY-WET differences

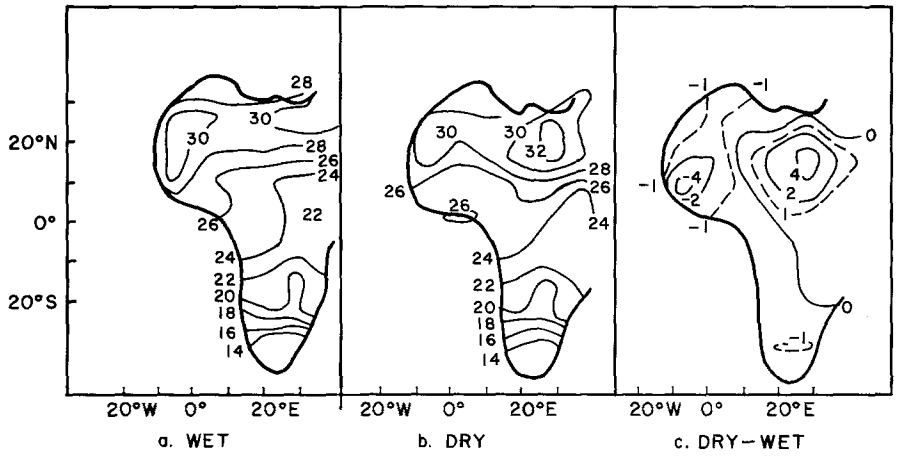

Fig. 4a—c. As in Fig. 3, but for surface air temperature (°C)

The ensemble characterized by sparse rainfall and less frequent cloudiness over northeast Africa experienced surface temperatures that were some 2—5°C higher than in the wet ensemble. The temperature differences, however, reversed sign along the northwest Atlantic coast where differences in precipitation rates and cloudiness were also reversed. Hourly diagnostics for the Sahel show that precipitation commences in late morning as surface temperatures rise above the threshold of moist convective instability. Higher surface temperatures in a moist atmosphere would therefore encourage more precipitation and clouds. The negative spatial correlation between surface air temperature and precipitation demonstrates that moisture deficits inhibited rainfall.

e) Humidity

Ensemble mean specific humidities at the surface over north Africa were, as expected, lower for the drought ensemble (not shown). More significantly, the precipitable water in the columns above the model Sahel were only 39—41 mm for the DRY years compared to 44—46 mm for the WET years. The surface relative humidity was much lower over the eastern half of the Sahel because of the combination of higher surface temperatures and lower absolute humidities. Surface heating under cloudless skies widens the gap between the available moisture and the moisture required for condensation and cloud formation, while frequent cloud cover helps to maintain moderate temperatures and near-saturation conditions. Trends in cloudiness and surface temperatures are thus mutually reinforcing.

f) Resultant surface winds

Figure 5 shows the surface circulation upstream of north Africa based on the resultant surface winds. Close inspection shows that the winds converging on western Africa that bring moisture to these regions were weaker in the drought ensem-

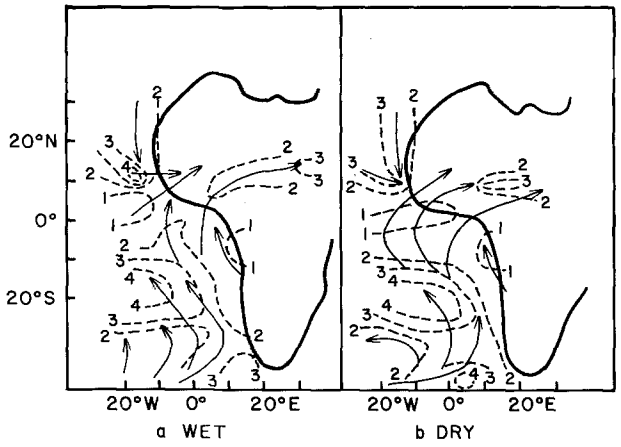

Fig. 5a, b. Direction and speed of the surface flow in August upstream of north Africa based on resultant winds. Isotachs are labeled in m s^{-1}

ble. The ensemble averages of the mean meridional component of the resultant surface wind (Fig. 6) show that somewhat greater mass convergence over the eastern Sahel occurs during drought than during rainier conditions, while the southerly flow bringing maritime air to northwest Africa (4° S to 4° N) is stronger for the rainy ensemble. Differences in these meridional winds are significant with about 94% confidence. Computations show that there is considerably more convergence of the northward momentum flux for these months over the coast of northwest Africa, where the moist flow from the South Atlantic Ocean crosses the equator and penetrates the continent. The SLP gradient immediately responsible for stronger northerly winds, and perhaps lower rainfall along 10° W, can be traced to lower SLP over northwestern Africa within the ITD and to higher SLP west of Gibralter over the Atlantic Ocean (Fig. 3). Comparison of the ensemble averages of the mean zonal component of the resultant surface wind did not reveal any noteworthy differences over Africa and adjacent Atlantic coastal waters.

Using monthly averaged quantities, it is difficult to establish whether initial anomalies in one particular synoptic field prompted the eventual divergence of the integrated local climate. For example, the resultant surface wind and mean surface specific humidity do not give any information regarding differences in the trends of the instantaneous moisture convergence during the month. However, a mutual consistency between the several fields can be cited. From what we have discussed above, we can suppose that the synoptic regimes of the drought months promoted lower levels of moisture convergence upstream of the Sahel and thereby stifled convective rainfall. The drier conditions, once established, led to higher temperatures, a deeper SLP trough and, consequently, greater mass convergence locally over interior north Africa.

g) Sea-surface temperature

The version of the model used here includes an interactive ocean whose surface temperature (SST) responds to changes in the air-sea energy budget. While the simulations do not give a completely accurate picture of atmospheric feedbacks on SST (because the model assumes prescribed ocean heat transports), it is not surprising that the mean SST were different for the two ensembles (Fig. 7). Mean SST for the rainy ensemble were more than 0.5° C cooler over a large part of the eastern North Atlantic Ocean. This ensemble also shows higher SLP in the same region (Fig. 3), referred to above in the explanation of computed

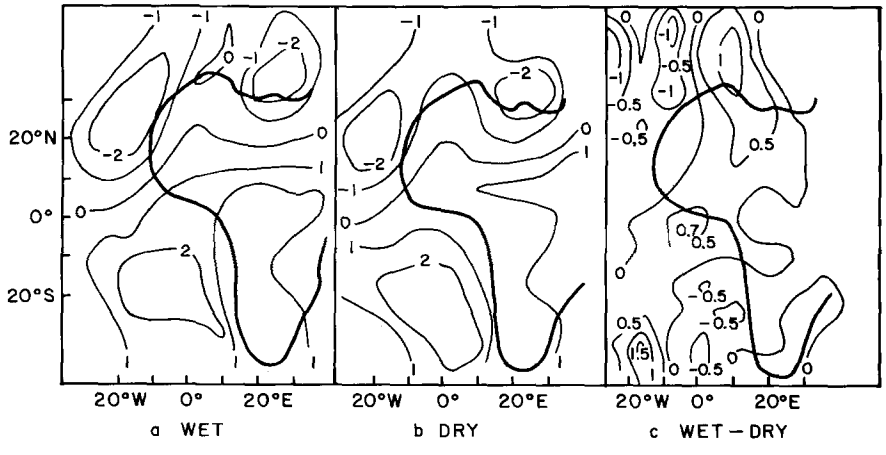

Fig. 6a—c. As in Fig. 3, but for the meridional component of the resultant surface wind. (m s^{-1})

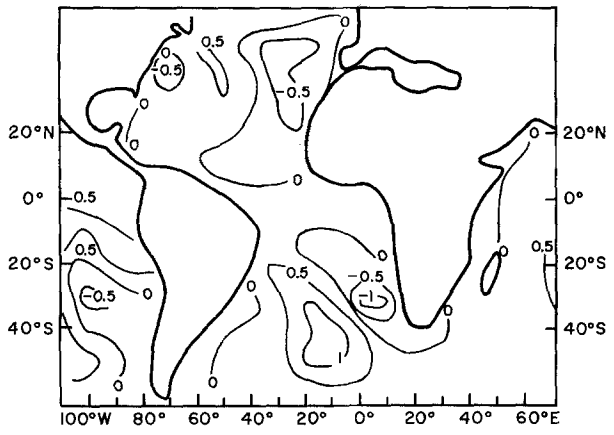

Fig. 7. WET-DRY differences in the August mean SST (°C)

dryness over northwest Africa. One can reason that a colder North Atlantic is conducive to a strong SLP high and therefore stronger northerlies that inhibit the penetration of southern hemisphere moisture into northern Africa. Here, however, these conditions seem to influence rainfall only over the northwest coast. Moreover, we recall the influence of the SLP distribution over north Africa on the circulation and note that it may be more important to the rainfall pattern than the strength of the subtropical anticyclones, as suggested, for example, by Lamb (1978).

The SST difference pattern between the drought and rainy ensembles over the southeast Atlantic Ocean is similar to Lamb's (1978) SST anomaly pattern. The DRY ensemble average SST range from 17.5—20° C within the usually cold tongue of the Benguela Current near South Africa while they have evolved to somewhat lower values (16—18° C) for the months with more copious Sahelian rainfall. Here, however, the maximum differences are a few deg latitude farther south than in Lamb's figure. They are comparable in magnitude to the model's standard deviations of SST, indicating that they make an important contribution to the model's interannual SST variability. Lamb's drought composite also shows anomalously warm SST adjacent to northwest Africa with a transition to colder water west of 23° W. The SST difference pattern between the DRY and WET model ensembles is in general agreement, indicating warmer water (23.5—25.0° C) for the DRY (versus 23.0—24.5° C for the WET) within the core of the Canary Current.

Other than their effect on the latitude of the ocean's thermal equator, and therefore the position of the ITCZ, is there a causal relationship between the aforementioned SST patterns and the actual or the simulated Sahelian rainfall deficits? More recent investigations (Lough 1986, Folland et al. 1986) have sustained the statistical link between warming in the South Atlantic Ocean and Sahelian drought, at least for the period 1948—1972. The first of these studies even determined that the southeastern Atlantic in particular is favored for SST maxima during such years. Both studies attribute the weaker SST/Sahel rainfall correlation of the first half of the 20th Century to the different spatial pattern of Sahel rainfall prevalent during droughts of those years (often characterized by wetter conditions over northwest Africa). The second study concludes that "... the SST anomaly pattern associated with Sahel drought is unlikely to be unique". This probably explains some of the discrepancies between the SST anomaly distributions found to be consistent with Sahel drought by studies based on data from different years. The drought ensemble of the present study also shows wet conditions over northwest Africa in this respect is different from actual droughts over the Sahel since 1970 and different too from the case studies by Lamb (1978) and Folland et al. (1986).

h) Global circulation

It has been suggested that Sahel drought is sometimes a local manifestation of anomalies in the general (global) circulation. Ensemble means of zonal averages were compared to determine if the two ensembles differ with respect to selected components of the general circulation. Some of the differences for latitudes 4° S—27° N may of course reflect the local drought/no drought differences over north Africa that were discussed above. Noteworthy differences in zonal means of the zonal component of the wind were found only at the surface: the WET ensemble mean surface speeds were slightly stronger, as westerlies along 12° N. and easterlies along the other latitudes between 4° S—27° N. These ensemble differences were not, however, statistically significant. Positive zonal means of the meridional component of the wind computed between 4° S—27° N at lower model levels and the surface are indicative of northward accelerations around the lower part of the southern Hadley cell. Here they are found to be consistently larger for the DRY ensemble to about 20° N, but then larger for the WET ensemble farther north, implying greater mass convergence for the DRY case at 20° N. Similarly, the return (southward) flow aloft is stronger in the

drought case at 16° N, but weaker at 23° N, implying greater divergence aloft during the DRY years. These ensemble differences in the zonal mean meridional wind are in the same sense as mass convergence differences noted over the Sahel; they are significant with better than 97% confidence at 23° N and with about 92% confidence at 16° N, based on a two-tailed t-test. As an additional indication of differences in the computed Hadley circulations, we note that the zonal mean mass streamfunction shows a slightly stronger rotation for the drought case, as well as larger zonal means of upward velocity from 12°—27° N.

The maximum zonal mean of precipitation at low latitudes is usually computed at 4° N or 4° S by the model for August. The ensemble mean of this maximum was about 8.7 mm higher for the WET case, representing a significant difference from the DRY ensemble with about 93% confidence. Weaker moist convection in the Dry case allows the stronger northward flow from the equator and contributes as well to the stronger upward motion noted above. No differences in zonal mean cloudiness occurred.

3 Pre-season development

a) Precipitation and humidity

Significant rainfall deficits over the Sahel actually persist in the drought ensemble during the three summer months, July—September (408 mm versus 587 mm). During May and June, Sahel rainfall is similar for both ensembles. The precipitation maximum of the northwest African monsoon moves northward during the spring and early summer, and Hastenrath (personal communication) has suggested that spring accumulations along the Gulf of Guinea coast may be positively correlated with subsequent mid-summer Sahel rainfall. The model simulations sustain this relationship in June but there are no differences in May and opposite sign differences in precipitation amount were computed at the coast for March and April.

Figure 8a—k show the chronological sequence of synoptic development that led to the simulation of a rainier summer over the Sahel in the WET ensemble runs. The higher rates of rainfall

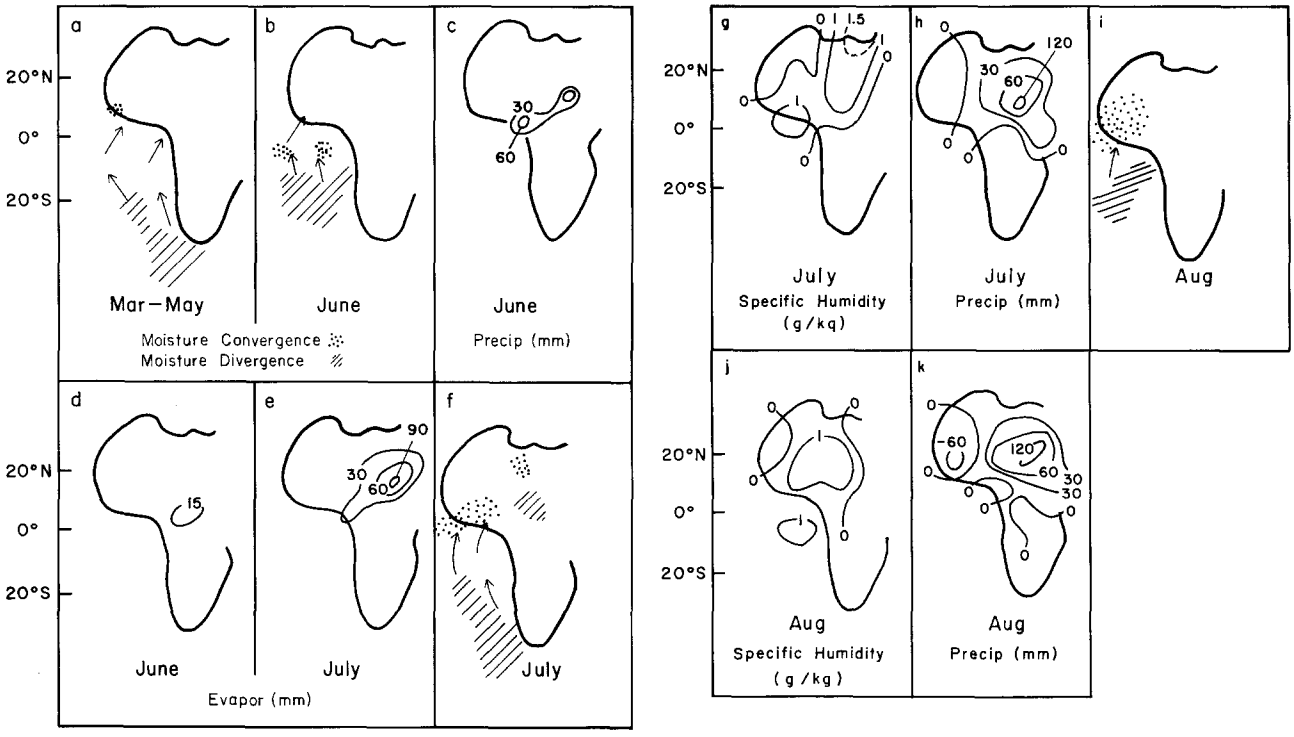

Fig. 8a—k. Sequence of synoptic events leading to contrasting July and August precipitation regimes over north Africa for WET and DRY ensembles. Each field represents WET-DRY differences in the seasonal or monthly means of the indicated meteorological variable

during July and August are associated with surface humidities that were at least 1g kg^{-1} higher during both months over much of north Africa and the Gulf of Guinea.

During March—May moisture was already being advected northward from the South Atlantic Ocean preferentially in the WET ensemble simulations (Fig. 8a). Fig. 8b shows that not only was more moisture transported out of the South Atlantic in June, but more moisture was converging over the Gulf in the WET ensemble than in the DRY case. The pattern of greater WET ensemble moisture divergence over the South Atlantic and greater moisture convergence over the Gulf continued into July except that the latter area moved northward (Fig. 8f). The additional ambient moisture of the WET case in July (Fig. 8g) and August (Fig. 8i) can be related to these areas of greater moisture convergence and greater evaporation. Large rainfall differences in July (Fig. 8h) and August (Fig. 8j) either coincide with or are immediately downwind of the area of large humidity differences. The WET moisture divergence over the eastern Sahel in July is probably a consequence of the evaporative cooling of the copious precipitation.

b) SST and circulation

Lamb (1978) and Lough (1986) found that the warm SST anomaly in the southeastern Atlantic may already appear during the spring months preceeding dry summers in the Sahel. However, no dynamic link is suggested between the warmth of the water and the eventual rain deficiency. Fig. 9a shows that the southeast Atlantic SST of the DRY ensemble were already higher in the spring, and

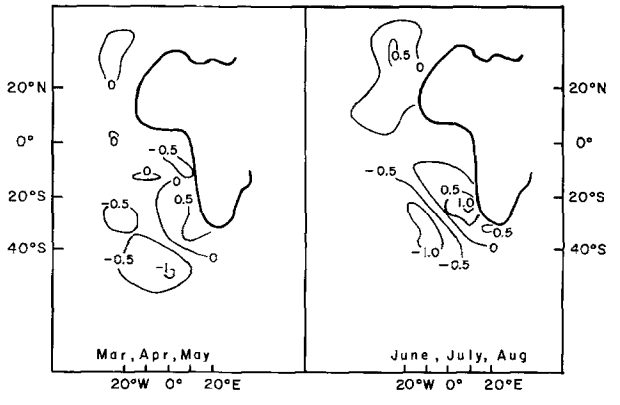

Fig. 9. DRY-WET ensemble difference seasonally averaged SST (°C)

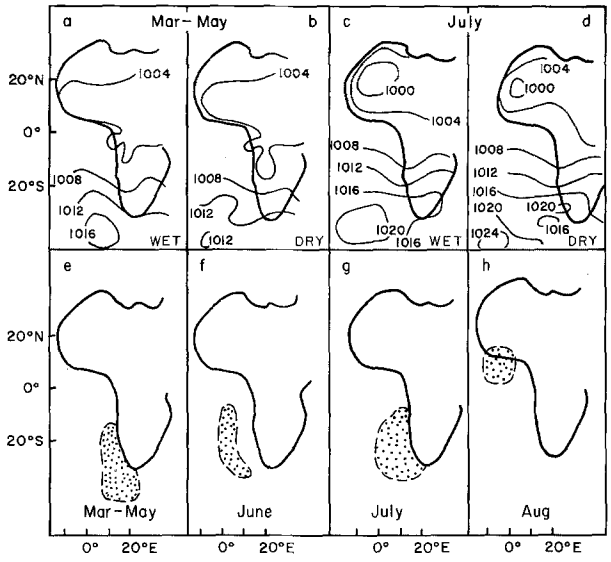

Fig. 10. a—d Distributions of SLP (mb); **e—h** Stipling indicates areas where southerly components of resultant surface winds were stronger in the WET ensemble than in the DRY ensemble

by June—August the SST difference in one area reached +1°C (DRY-WET) (Fig. 9b). Over mid-ocean, even larger opposite sign SST differences persist from January—August. Maximum differences in the ensemble mean SST in the South Atlantic for each of these months are at least as large as standard deviations of the model's computed monthly mean SST. In general, DRY ensemble SST isotherms over the extratropical South Atlantic Ocean were more zonal than in the WET ensemble. Differences in the ensemble mean evaporation rates over the South Atlantic were distributed such that lower SST corresponded with higher rates of evaporation, reflecting the dominant role of latent heat flux in determining SST trends.

The DRY ensemble SLP were lower over the southeastern Atlantic Ocean (near the warmer water) until August (Fig. 10a—d). An SLP maximum did develop in June, but farther southwest (closer to the cooler water), and persisted through August. The higher SLP of the WET ensemble created stronger pressure gradients and consequently stronger southerly winds over the southeast Atlantic (Fig. 10e—h). These, in turn, increased the rate of upward latent heat flux from the ocean surface, compared to the DRY ensemble, and contributed to the persistance of colder SST near southwest Africa. Undoubtedly, these stronger southerly winds are responsible for the greater moisture advection from the southeast At-

lantic toward north Africa that is apparent in Fig. 8a, b, f and i.

4 Summary and discussion

A 37-year simulation of global circulation and climate shows considerable interannual variation of precipitation over the African Sahel. The model includes an interactive ocean so that interannual variations of sea-surface temperature (SST) also occur. August rainfall computed for the sub-Sahara for five "drought" (DRY) years was only about 60% of the August rainfall for five WET years.

Higher SLP overlying slightly cooler SST in the North Atlantic, coupled with lower pressures over northwest Africa, gave stronger northerlies during the WET August, and this may have contributed to the low precipitation accumulations along the North Atlantic coast of Africa. These synoptic conditions appear not to have influenced the rainfall computed for the central or eastern Sahel.

The meridional rotation of the southern Hadley cell was slightly stronger for the DRY ensemble, as were meridional accelerations and upward velocities south of 20° N. Excess moist convection during the WET years near the equator undoubtedly slowed the thermal forcing that drives the cell. The stronger Hadley cell of the DRY ensemble is not consistent with the lower moisture convergence over north Africa that characterized the simulated drought, so that global-scale circulation anomalies cannot be cited among the causes of the drought in these model simulations.

The foregoing discussion describes how several consequences of drought conditions were reflected by the concurrent mean synoptic fields. Although one may assume that the immediate cause of the infrequent moist convection was the low concentration of atmospheric moisture, the August synoptic fields did not unequivocally indicate the circulation characteristics responsible for this condition.

These computer simulations, as well as previous observational studies, showed that dry summers in the Sahel are often preceded by several months of anomalously warm SST in the southeast Atlantic Ocean. The simulations suggest that the warmer temperatures may weaken the high pressure and thereby cause slackening of the southerly winds that transport moisture toward north Africa. A positive feedback can set in since low wind speeds inhibit the upward flux of latent heat, keeping the SST warm. In any case, in these simulations and perhaps also in nature, it is the less efficient advection of moisture from the southeast Atlantic Ocean, perhaps as early as March and until the beginning of the Northern Hemisphere summer, that is responsible for the sparsity of precipitation over north Africa.

Were the differences in the SLP distributions spurred by the differences in the SST patterns or were the latter primarily a result of atmospheric circulations that developed differently for other reasons? The persistance of the pattern of SST differences from January—August over the South Atlantic Ocean lends support to the first premise. Moreover, the SLP maxima were usually above or slightly southwest of the areas of colder water. Note, however, that the lower SST of the WET ensemble near southwest Africa were consistent with the stronger cold advection implied by the surface winds and that the warmer SST were perhaps reinforced by additional warm air advection west of the high centers that were present in March—May and July.

Results suggest that initial SST anomalies can instigate atmospheric circulations that are mutually reinforcing, allowing the SST anomalies to persist for many months. If such a circulation is conducive to regional drought, the latter may be predictable months in advance.

Simulation experiments in which SST anomalies are prescribed could be profitably employed to clarify the sensitivity of the model's computation of Sahelian rainfall to the lower boundary conditions over the South Atlantic Ocean. It remains to be seen whether the interannual variation of SST explain enough of the variance of Sahel precipitation to be useful as predictors.

Acknowledgements. Technical assistance for data processing required by the research was arranged through the cooperation of Dr. G. Russell. Dr. D. Rind provided welcome encouragement during the research and during the preparation of the manuscript, offering valuable suggestions and insight into the challenges presented by the study.

References

Chervin R, Druyan L (1984) The influence of ocean surface temperature gradient and continentality on the Walker circulation. Part I: Prescribed tropical changes. Mon Wea Rev 112: 1510—1523

Dennett M, Elston J, Rogers J (1985) A reappraisal of rainfall trends in the Sahel. J Climatol 5: 353—361

Druyan L (1982a) Studies of the Indian summer monsoon with a coarse-mesh general circulation model, Part I. J Climatol 2: 127—139

Druyan (1982b) Studies of the Indian summer monsoon with a coarse-mesh general circulation model, Part II. J Climatol 2: 347—355

Folland C, Palmer T, Parker D (1986) Sahel rainfall and worldwide sea temperatures, 1901—85. Nature 320: 602—607

Hansen J, Russell G, Rind D, Stone P, Lacis A, Lebedeff S, Ruedy R, Travis L (1983) Efficient three-dimensional global models for climate studies: models I and II. Mon Wea Rev 111: 609—662

Hansen J, Lacis A, Rind D, Russell G, Stone P, Fung I, Ruedy R, Lerner J (1984) Climate sensitivity: an analysis of feedback mechanisms. Climate Processes and Climate Sensitivity, Geophysical Monograph 29, Maurice Ewing Vol. 5, Amer Geophys Union, 130—162

Kidson J (1977) African rainfall and its relation to the upper air circulation. Quart J R Met Soc 103: 441—456

Lamb P (1978) Large-scale tropical Atlantic surface circulation patterns associated with Subsaharan weather anomalies. Tellus 30: 240—251

Lough J (1986) Tropical Atlantic sea surface temperatures and rainfall variations in Subsaharan Africa. Mon Wea Rev 114: 561—570

Miller J, Russell G, Tsang L (1983) Annual ocean heat transports computed from an atmospheric model. Dyn Atmos Oceans 7: 95—109

Newell R, Kidson J (1984) African mean wind changes between Sahelian wet and dry periods. J Climatol 4: 27—33

Nicholson S (1980) The nature of rainfall fluctuations in subtropical West Africa. Mon Wea Rev 108: 473—487

Nicholson (1981) Rainfall and atmospheric circulation during drought periods and wetter years in West Africa. Mon Wea Rev 109: 2191—2208

Stone P, Chervin R (1984) The influence of ocean surface temperature gradient and continentality on the Walker circulation. Part II: Prescribed global changes. Mon Wea Rev 112: 1524—1534